AJAE

Open Access

Vol. 14, No. 3, pp. 289-306, September 2020
doi: https://doi.org/10.5572/ajae.2020.14.3.289
ISSN (Online) 2287-1160, ISSN (Print) 1976-6912

Research Article

Annular Solar Eclipse on 26 December 2019 and its Effect on Trace Pollutant Concentrations and Meteorological Parameters in Kannur, India: a Coastal City

Resmi CT[1)], Nishanth T[2),*], Satheesh Kumar MK[3)], Balachandramohan M[1)], Valsaraj KT[4)]

[1)]Department of Physics, Erode Arts and Science College, Tamil Nadu, India-638009
[2)]Department of Physics, Sree Krishna College Guruvayur, Kerala, India-680102
[3)]Department of Atomic and Molecular Physics, Manipal Academy of Higher Education, Karnataka, India-576104
[4)]Cain Department of Chemical Engineering, Louisiana

***Corresponding author.**
Tel: +91-9895415281
E-mail: nisthu.t@gmail.com

Received: 26 May 2020
Revised: 27 July 2020
Accepted: 1 August 2020

ABSTRACT This paper highlights the variations of surface ozone (O_3), total column ozone (TCO), oxides of nitrogen (NO and NO_2), carbon monoxide (CO), sulphur dioxide (SO_2), ammonia (NH_3), volatile organic compounds (Benzene, Tolune, Ethyle Benzene, Xylenes (collectively called BTEX)), particulate matters (PM_{10} and $PM_{2.5}$), and meteorological parameters at the time of an annular solar eclipse on 26 December 2019 at Kannur town in Kerala, South India. The maximum solar obscuration has resulted a decrease in solar radiation by 93%, air temperature by 16.3%, wind speed by 36.1% and an increase in relative humidity by 27.1% at this coastal location. Along with the reduction in solar radiation, the concentration of surface O_3 (61.5%) and total column O_3 (11.8%) have been observed to decrease at the maximum phase of solar eclipse. CO and NO_2 concentration were found to be increased by 28.9% and 42.2%, respectively, while NO exhibited its typical diurnal variation. Further, a decrease in concentrations of SO_2 by 17.6%, PM_{10} by 18.5%, and $PM_{2.5}$ by 11.3% were observed. NH_3 and BTEX were found to be higher than 11.3% and 22.6% of the concentrations in control days. All of these deviated parameters could be seen returning to their normal state after completing the eclipse episode. The variation of photodissociation coefficient j(NO_2) values were theoretically calculated from the observed data, which shows a good agreement with the model simulated j(NO_2) reduction. This is an extensive second observation on the variation of trace pollutants on solar eclipse, after the partial solar eclipse observed on 15 January 2010 at Kannur.

KEY WORDS Solar eclipse, Kannur, Air pollutants, Surface O_3, Model simulations

1. INTRODUCTION

Solar eclipse is a natural phenomenon that provides a distinct reduction of solar radiation for a fixed duration due to the obscuration of the solar disc by the moon. Being a rare astronomical event, it provides a unique occasion to investigate the spontaneous changes in photochemistry, dynamics, and boundary layer height (BLH) in the atmosphere due to the variations in the ascending and descending phases of solar radiation (Stoev *et al.*, 2005; Szalowski, 2002; Koepke *et al.*, 2001; Winkler *et al.*, 2001; Fernandez *et al.*, 1996; Manohar *et al.*, 1995). Several investiga-

tors have reported the effects of various atmospheric parameters at the time of a solar eclipse in different parts of the globe (Gröbner *et al.*, 2017; Dutta *et al.*, 2011; Krezhova et al., 2008; Aplin and Harrison, 2003; Dolas *et al.*, 2002; Foken *et al.*, 2001; Vogel *et al.*, 2001; Hanna, 2000; Prenosil, 2000; Anderson, 1999; Eaton *et al.*, 1997; Segal *et al.*, 1996). Various researchers have explored the pronounced variations in the atmospheric boundary layer (ABL) height at the eclipse event (Ratnam *et al.*, 2010; Founda *et al.*, 2007; Krishnan *et al.*, 2004; Kapoor *et al.*, 1982; Raman, 1982). Subrahamanyam *et al.* (2012) observed a double mixed boundary layer between 700 and 1500 m during the solar eclipse on 15 January 2010 at Thiruvananthapuram, which was due to the horizontal advection of air mass. The atmospheric turbulence decay during the total solar eclipse of 11 August 1999 was examined by Anfossi *et al.* (2004), and their observations were in good agreement with the theoretical model of turbulence decay.

Studies were focused on the eclipse induced surface air temperature variations and reported a sharp decrease in air temperature at the maximum phase of the eclipse (Calamas *et al.*, 2019; Nymphas *et al.*, 2009; Kolarz *et al.*, 2005; Krishnan *et al.*, 2004; Sethuraman, 1982). Wang and Liu (2010) observed a warming of 7°C at 17 km altitude due to thermal contraction, and cooling of 2°C in the troposphere due to reduction in solar heating during the total solar eclipse on 22 July 2009. Likewise, a temperature reduction of 2°C was observed around the tropopause over Thumba by Subrahamanyam *et al.* (2011) at the annular solar eclipse of 2010, and revealed that these changes were associated with a significant reduction in turbulent kinetic energy, momentum flux, and sensible heat flux at the peak period of the eclipse. Observations of land surface temperature changes over Europe during the total solar eclipse on March 2015 by Elizabeth (2016) found to drop up to several degree Celsius, and this temperature drop was correlated with solar intensity variation. Muraleedharan *et al.* (2011) reported an abnormal warming in the upper troposphere due to decrease in tropopause height on the solar eclipse day 2010 at Goa, India.

Generally, humidity increases with the reduction in surface air temperature (Bhat and Jagannathan, 2012), and this cooling alters the stability of boundary layer in the lower atmosphere (Gorchakov *et al.*, 2008; Praveena *et al.*, 2004). Jokinen *et al.* (2017) identified the formation of new particles caused by aerosol loading and lack of oxidized organic compounds during the solar eclipse in 2015. Apart from the variations observed in meteorological parameters and atmospheric dynamics, solar eclipses induced substantial impact on the stratospheric and surface O_3 photochemistry, and several studies have been carried out in this direction (Gerasopoulos *et al.*, 2008; Zanis *et al.*, 2007; Tzanis, 2005; Fabian *et al.*, 2001). Observations of total column O_3 using ground based devices during eclipse events by different groups show a decrease in O_3 concentration during the maximum phase of eclipse (Chudzynski *et al.*, 2001; Zerefos *et al.*, 2000; Mims and Mims, 1993).

As the sunlight is obscured for few minutes, the weather parameters fluctuate, resulting in a drastic change in the concentrations of atmospheric O_3 and nitrogen dioxide (Amiridis *et al.*, 2007; Fabian *et al.*, 2001). Manchanda *et al.* (2012) have reported a decrease in the O_3 concentration in the stratosphere and troposphere instantly after the maximum phase of the eclipse due to temperature cooling, on the solar eclipse of 15 January 2010 at Thiruvananthapuram. Only very few studies have been reported on the changes in the surface O_3 and their photochemistry during the eclipse event in India (Girach *et al.*, 2012; Reddy *et al.*, 2012; Vyas *et al.*, 2012; Nishanth *et al.*, 2010; Sharma *et al.*, 2010; Naja and Lal, 1997; Srivastava *et al.*, 1982). In addition, they also validated the model simulation response, which was in agreement with the observed effect.

This is the second study on the variation of air pollutants on solar eclipse, after the partial solar eclipse observed on 15 January 2010 at Kannur; in which we could investigate the variations of surface O_3, NO_x and meteorological parameters at Kannur University campus. Here we describe the results on the variation of surface O_3, NO, NO_2, CO, SO_2, NH_3, particulate matters (PM_{10} and $PM_{2.5}$), Volatile Organic Compounds include Benzene, Tolune, Ethyle Benzene, Xylenes (collectively called BTEX), total ozone column (TOC) and meteorological parameters (total solar radiation, temperature, relative humidity, wind speed and wind direction) at Kannur Town. Further, a detailed account of the inter-correlation between observed trace pollutants and meteorological parameters is discussed. In addition to these, theoretical calculation and model simulation for the photodissociation coefficient j(NO_2) is discussed in this paper. This investigation shows that at Kannur town, which is highly polluted than Kannur University Campus, the synoptic movement of atmospheric trace species plays a crucial

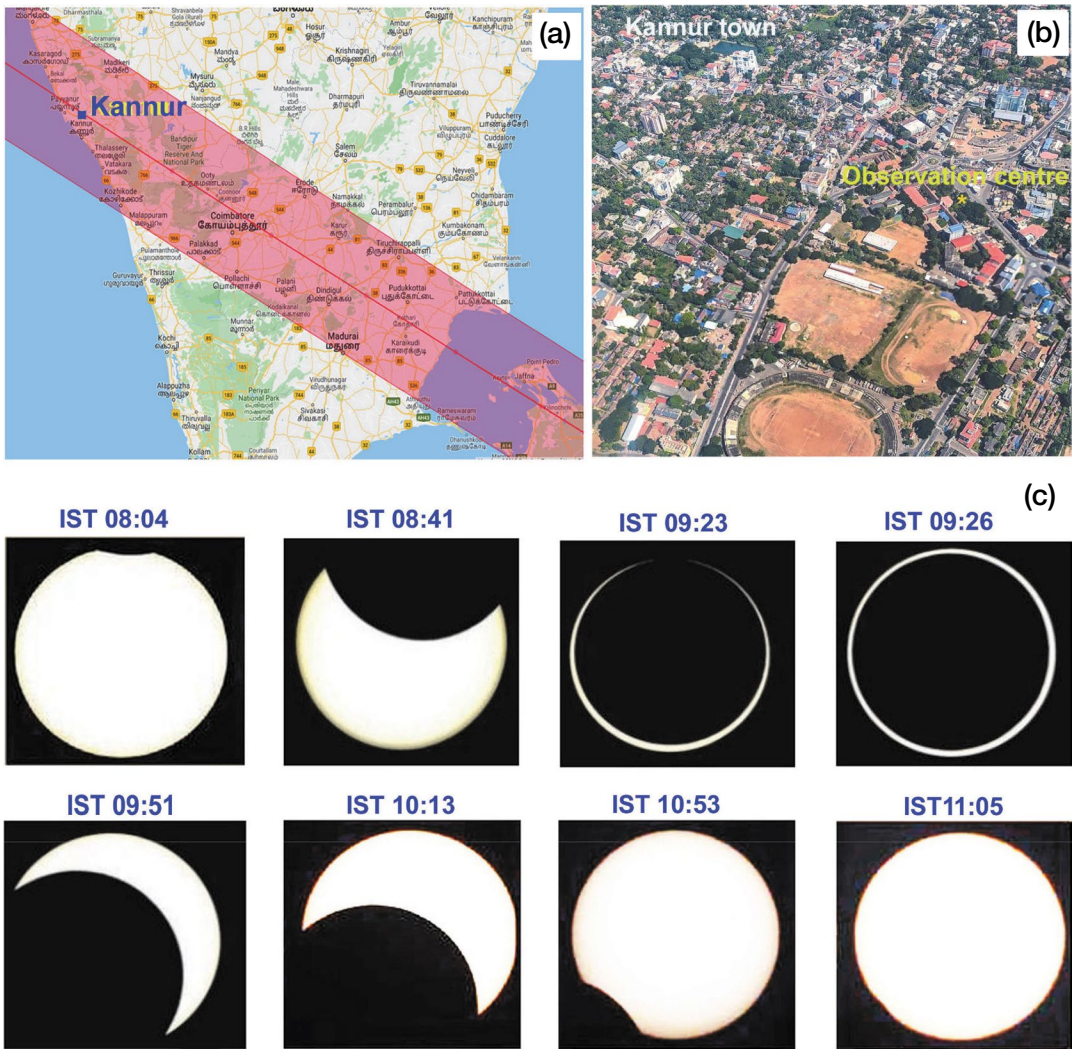

Fig. 1. (a) Eclipse path passing over Indian region (source: NASA tracks the path of the annular eclipse on Google Maps), (b) aerial view of observation centre and surroundings at Kannur town, (c) timings for the annular solar eclipse viewed from Kannur (The image taken by using Canon EOS 6D Mark II Camera).

role in the progress of eclipse induced changes in the surface O_3 and other trace pollutant.

2. METHODS

2.1 Description of the Eclipse

The annular solar eclipse is a phenomenon in which the sun is partially or completely obscured when the moon comes between the sun and earth, causing the sun's outer surface appears as a ring. The annular solar eclipse of December 26, 2019 started from Hofuf in Saudi Arabia, Qatar, and UAE. It was then crossed over India, Sri Lanka, Malaysia, Indonesia, Singapore, and ended at Guam in the China Sea. Fig. 1(a) shows the path of solar eclipse over Indian region. At Kannur, the annular solar eclipse began at 08:04 IST, reached total obscuration at 09:26 IST and completed at 11:05 IST. The total eclipse lasted for 3 minutes and 12 seconds with a magnitude of 0.98, when the Moon came close to the centre of the Sun. The duration of the eclipse was 3 Hrs 1 minute at Kannur.

2.2 Observational Site

Kannur is the northern district of Kerala state, lying between the Arabian Sea coast in the west, and Western

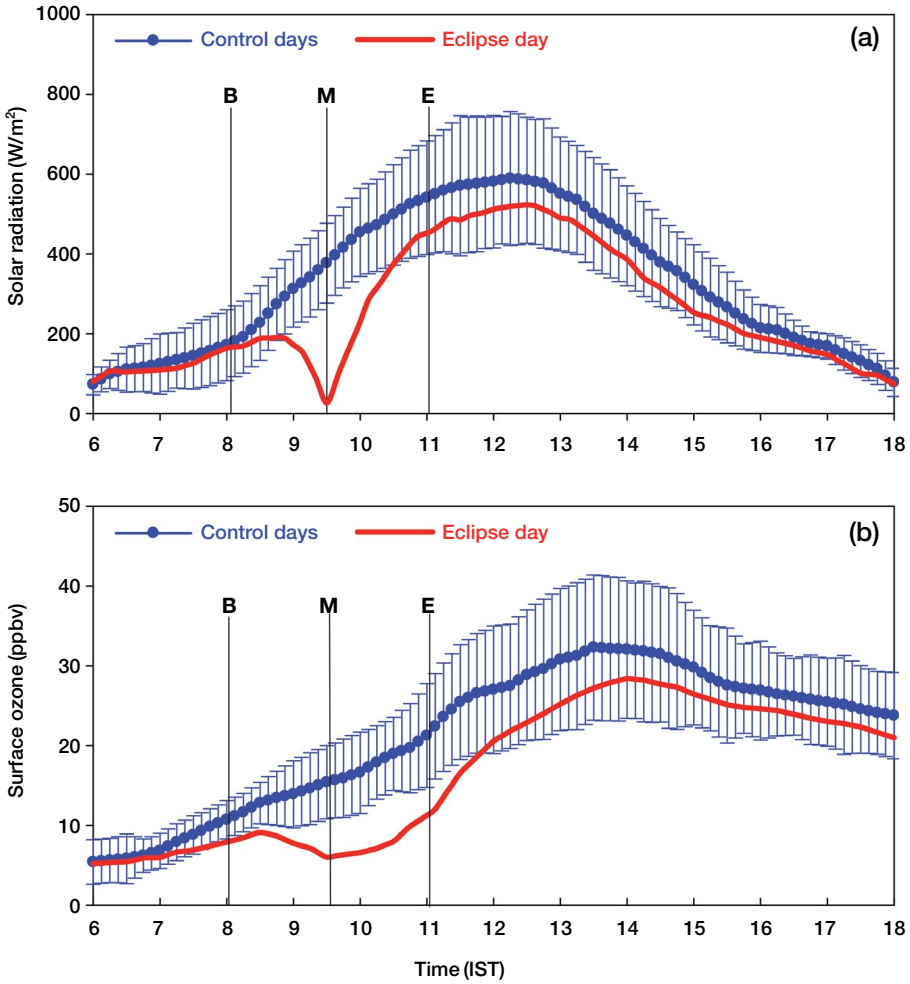

Fig. 2. Variations of (a) solar radiation and (b) surface O_3 observed during eclipse day and control days.

Ghats mountain ranges in the east. Kannur is the sixth-most urbanized district in Kerala, and is one of the most popular tourist destinations in South India. It is a semi urbanized city having few industries including plywood, rub wood, mattress factories, and handloom, while agriculture and fisheries are the key sectors in villages of this district. The observational site is close to the National Highway (NH 17) as shown in the Fig. 1(b), which has reasonably heavy traffic during the day and minimum at night. The observational site is surrounded by commercial buildings and residential area, and is about 2 km away from the Arabian Sea. Since the industries are quite far, vehicular emission is the major source of air pollution at this site. Ground based observations were performed continuously from 23 to 29 December 2019 at Kannur town (11.87°N, 75.37°E, 3 m msl) to measure the concentrations of trace gases and particulate matters in the wake of the solar eclipse on 26 December. Kannur district was identified the location in the Indian sub-continent where this annular solar eclipse was first observed. The timings for the solar eclipse viewed over Kannur is shown in the Fig. 1(c). As the eclipse occurred in winter season, the environment was less humid with clear sky and wind was from north-west at this site.

2.3 Experimental Setup

Measurements of trace pollutants were carried out using the respective ground based gas analyzers from Environment S.A France. The measurements of surface O_3 were made using a continuous O_3 analyzer (Model O342e) with a detection limit of 0.2 ppbv. Its working principle is based on O_3 detection by direct absorption in UV light. O_3 absorption spectrum is intense in the 250 and 270 nm wavelength range. Thus, it corresponds to

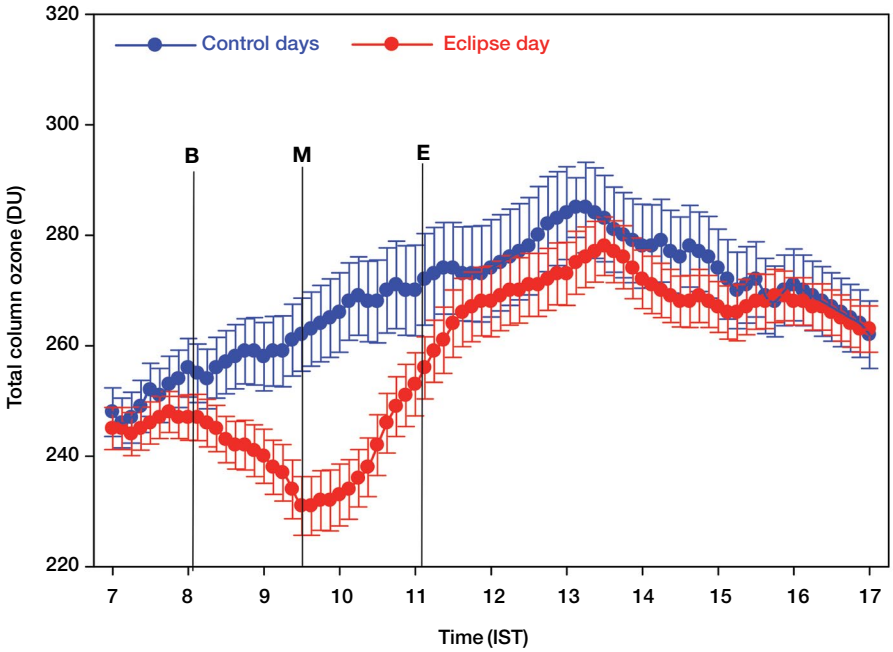

Fig. 3. Variation of total column O_3 for control days and the eclipse day.

the maximum range of O_3 absorption at 255 nm.

Total column O_3 (TCO) concentrations and the variations in solar UV radiation were recorded at regular intervals using the Microtop II ozonometer (Solar Light Co., Inc, USA). The MICROTOPS-II consists of two sets of instruments, namely sun photometer for aerosol optical depth measurement at five discrete wavelengths and an ozonometer, for measuring the total column O_3 (TCO) using three UV channels. This sun photometer measures the total O_3 at three different wavelengths 305.5, 312.5 and 320 nm in the UV region of the solar spectrum by using differential optical spectroscopic technique.

NO, NO_2 and NH_3 were measured with the aid of gas analyzer (Model AC32e) with a detection limit of 0.2 ppbv. Its working principle is based on the NO chemiluminescence in the presence of highly oxidizing O_3 molecules. The NO in the ambient air is oxidized by O_3 to form excited NO_2 molecules. The concentrations of NO, NO_2 were measured based on the spectrum of the radiation emitted by NO_2 molecules at the excited level. Particulate matters (PM_{10} and $PM_{2.5}$) were measured by using suspended particulate beta gauge monitor (Model MP101M). Its working principle is based on the particle measurement by beta radiation attenuation. The measurement consists of calculating the absorption difference between a blank filter and a loaded filter, knowing that the beta ray absorption follows an exponential law and is independent of the physiochemical nature of the particles.

Measurements of CO were made by using an analyzer (Model CO12e) with a detection limit of 0.05 ppm. Its working principle is based on CO detection by absorption in infrared light. VOC's (BTEX) were measured, based on gas chromatography coupled with a PID detector by using (VOC72e) analyzer. SO_2 measurements were made by using a UV fluorescent Sulfur dioxide analyzer (Model AF22e) with a detection limit of 0.4 ppbv. The ambient air to be analysed is filtered by a hydrocarbon removing aromatic molecule device. The hydrocarbon molecule free sample to be analysed is sent to a reaction chamber, to be irradiated by an UV radiation centred at 214 nm, which is the SO_2 molecule absorption wavelength. All the gas analyzers have been calibrated by using sample gases on a regular basis. The total solar radiation was measured by LSI LASTEM Italia (DPA870) pyranometer and surface air temperature measured by an external Pt100 sensor.

3. RESULTS AND DISCUSSION

3.1 Variation of Solar Radiation, Surface and Total Column O_3

In order to study the influence of solar eclipse on the

variation of air pollutants over Kannur, the study period was divided into two spans; viz., eclipse day (26 December 2019) and control days (pre-eclipse days of December 23, 24, 25 and post-eclipse days of December 27, 28, 29). Fig. 2 shows the day time variations in (a) solar radiation, and (b) surface O_3 at the observational site on the solar eclipse day and the control days. The error bars in the figure shows a standard deviation in the respective parameter for 6 control days. The beginning, maximum and the end of the solar eclipse are marked as B, M and E in the figure with vertical lines. The figure displays a steady decrease in solar insolation observed from 08:04 IST and became minimum during the maximum obscuration at 09:26 IST, and then started increasing.

The intensity of solar radiation regained its normal value by the end of the eclipse (11:05 IST). It was found that the intensity of solar radiation declined from $376 \pm 101\,Wm^{-2}$ (average value on control days) to $26\,Wm^{-2}$ on the eclipse day at 9.26 IST with a reduction of 93%. Likewise, surface O_3 concentration started to decrease from 9.3 pbbv at the beginning of the eclipse (08:15 IST) and reached its minimum value of 6.5 ppbv at 09:26 IST, and after full obscuration it started to increase till the end of the eclipse. During control days and eclipse day, surface O_3 concentration reaches its peak value at the noon time, 30 minutes after the maximum intensity of solar radiation, while the O_3 decline was in phase with solar radiation on eclipse day. Thus, a sharp decrease in O_3 concentration (61.5%) was noticed during the maximum phase of the eclipse at 09:26 IST when compared to the respective values in the control days. This decline of O_3 was due to the slow rate of photolysis of NO_2 in the declining phase of the solar intensity as shown in the figure. This is in tune with the similar observations at the maximum phase of solar obscuration during the eclipse on 15 January 2010, at Kannur University campus (Nishanth *et al.*, 2011), and at Thiruvananthapuram (Girach *et al.*, 2012).

Studies carried out at various locations during different solar eclipses have shown different magnitudes of change in the concentration of surface O_3. Naja and Lal (1997) have observed a decrease of 18–21% at Ahmedabad during the solar eclipse of 24 October 1995 and Abram *et al.* (2000) have reported a decrease of 8% of O_3 at Silwood Park, Ascot during the solar eclipse of 11 August 1999. Tzanis *et al.* (2008) have observed a higher rate of change O_3 one hour after the maximum phase of the solar obscuration over four observation centres in Greece during the solar eclipse of 29 March 2006.

The day time variations of total column O_3 on the eclipse day and the control days are shown in Fig. 3. Column O_3 concentration was found to increase during day time when photochemical reactions occurs in the presence of solar radiation, N_2O_5, and nitrogen oxides such as NO, NO_2 and NO_3 (Kostadinov *et al.*, 1999). Actinic flux in troposphere may have a strong reduction by stratospheric O_3 absorption by which photochemistry in the troposphere depends on stratospheric O_3 concentrations (Madronich and Flocke, 1999). In high NO_x environments, higher photo-dissociation rate coefficients (j) result in tropospheric O_3 production; while in low NO_x regions, O_3 destruction is enhanced (Fuglestvedt *et al.*, 1995; Madronich and Granier, 1992; Liu and Tranier, 1988).

The average concentration of total column O_3 varied between 248 ± 4.4 to 285 ± 8.2 DU during control days, and it showed a lower concentration on eclipse day. From the figure, it is clear that the total column O_3 concentration was found to be decreasing from the beginning of the eclipse (08:04 IST) and reached the minimum during the maximum phase of the eclipse and then returns to normal value after the eclipse event. With respect to control days, TCO was decreased from $262 \pm 6.6\%$ to $231 \pm 5.3\%$ in a time of 10 minutes after the maximum phase of solar obscuration. Thus, a change of 31 DU which correspond to 11.8% change in TCO was observed. A similar variations were reported at Thiruvananthapuram (Kumar *et al.*, 2014) and New Delhi (Chakrabarty *et al.*, 2001) during the eclipse events in 2010 and 1995. Chakrabarty *et al.* (1997) observed a sharp decrease in total column ozone before 10 minutes of maximum obscuration of the Sun over Ahmedabad during the solar eclipse of 1997. Using MICROTOPS Sun photometer, Kazadzis *et al.* (2007) reported that a decrease in 30–40 DU total column ozone in Kastelorizo, Greece on the day of eclipse on 29 March 2006. The measurements of total column ozone using MICROTOPS II Ozone Monitor by Girach *et al.* (2012) show a decrease of 14 DU at the maximum phase of eclipse at Thiruvananthapuram during 2010. Further they observed a fluctuation of columnar ozone about 20 minutes after the maximum phase of eclipse due to the presence of wave activity. Thus, the observed variation in TCO over Kannur, during the eclipse needs a detailed investigation incorporating fluid dynamics, and photochemical models to explore the boundary layer dynamics and associated vertical mixing.

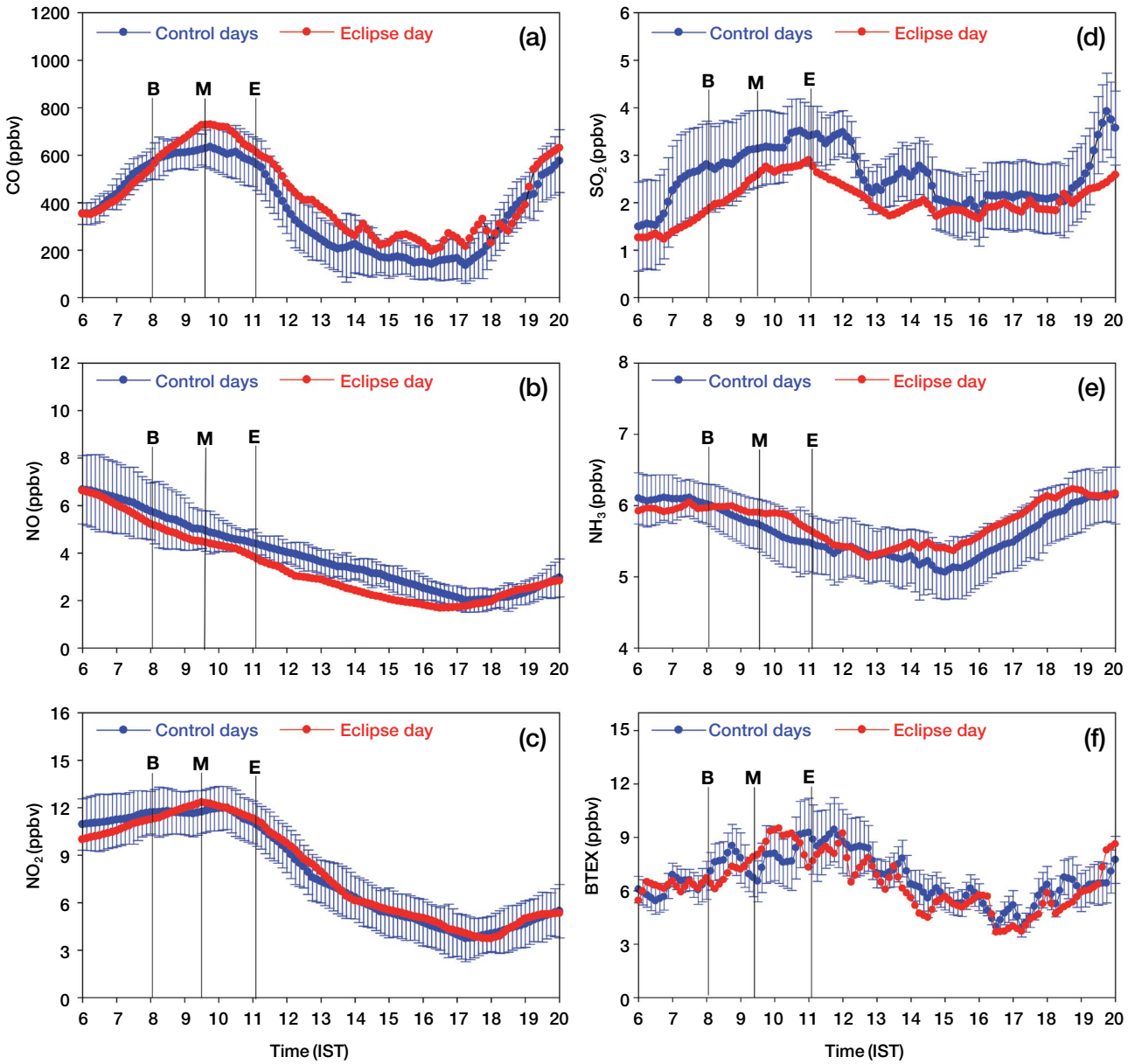

Fig. 4. Variations of (a) CO, (b) NO, (c) NO_2, (d) SO_2, (e) NH_3 and (f) BTEX observed during eclipse day and control days.

3.2 Variations of CO, NO, NO_2, SO_2, NH_3 and BTEX

Diurnal variations of CO and NO_2 usually exhibited two maxima during morning and evening due to peak traffic hours at Kannur town. Generally, the morning peak occurred at 10:00 IST and evening peak at 20:00 IST. The observed low concentrations during the day time hours and high concentrations during the night time hours are mainly due to the local emissions and the boundary layer height variations. Since CO and NO_2 are the prominent precursors of O_3, their concentrations were found to be lower in the afternoon (around 14:00 IST) when O_3 concentration became a maximum. Several researchers reported a similar diurnal variation O_3 and its precursors in many urban areas in India (Verma *et al.*, 2017; Mahapatra *et al.*, 2014; Beig *et al.*, 2007; Naja and Lal, 2002).

The day time variations of CO, NO and NO_2 for control and eclipse days are shown in the Fig. 4(a, b, c), respectively. During control days, the concentration of

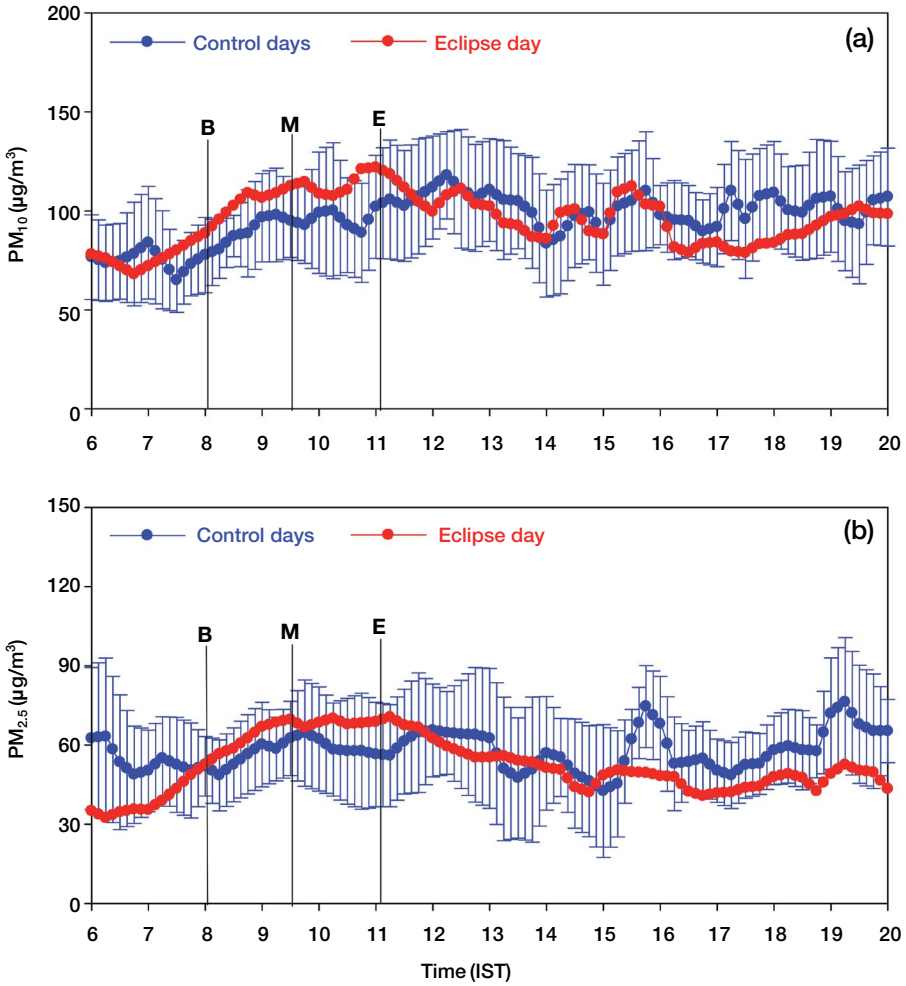

Fig. 5. Variations of (a) PM_{10}, (b) $PM_{2.5}$ observed during eclipse day and control days.

CO varied from 140 ± 56 to 633 ± 145 ppbv, and that of NO and NO_2 varied from 2.01 ± 0.58 to 6.78 ± 1.44 ppbv, and 3.34 ± 1.1 to 10.54 ± 1.2 ppbv, respectively. This clearly indicates the photochemical production of O_3 in the presence of NO_2 from CO, CH_4 and VOC's (Nair *et al.*, 2018; Tyagi *et al.*, 2016; Nishanth *et al.*, 2014). A considerable reduction in solar radiation during the eclipse delayed the atmospheric chemical reactions which resulted in a reduced photochemical production of surface O_3 by NO_2. The instant consequence of eclipse is earmarked by a decline in j(NO_2) in tune with the in solar radiation. Thus, the theoretical calculation along with a photochemical box model simulation were used to determine the j(NO_2) variation for control and eclipse days and the details are discussed in section 3.6.

An increase in CO concentration was observed from the beginning of eclipse (590 ppbv), and it reached a maximum value (728 ppbv) during the maximum obscuration. Thus, a sharp increase in CO concentration (28.9%) was observed during the maximum phase of the eclipse (09:26 IST) when compared to the respective time in the control days. Further, the concentration of NO_2 was found to be increased by 42.2% during the maximum phase of the eclipse with respect to control days, while NO concentration remained unchanged during the maximum phase of the eclipse. Similar variation of NO, NO_2 and CO were observed at Thumba in Thiruvananthapuram (Girach *et al.*, 2012) and Mangattuparamba in Kannur (Nishanth *et al.*, 2010) during the eclipse in 2010. This increase in NO_2 and CO may be influenced by the geography, morning traffic and it may have significant influence on the variation of boundary layer dynamics. This needs to be analysed in detail with the aid of spatially separated observations during the

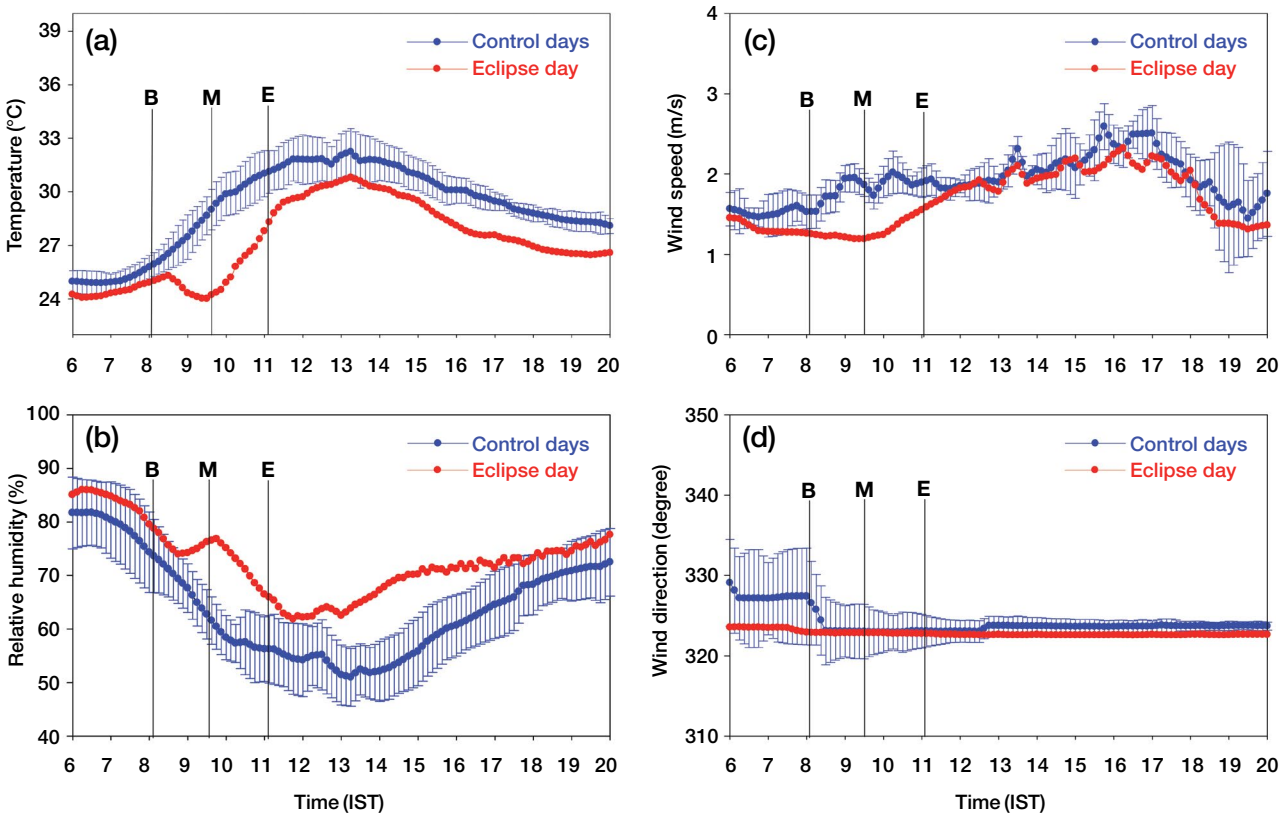

Fig. 6. Variations of (a) temperature, (b) relative humidity, (c) wind speed, (d) wind direction observed during eclipse day and control days.

eclipse.

The day time variations of SO_2, NH_3 and BTEX for control and eclipse days are shown in the Fig. 4(d, e, f), respectively. The diurnal variation of SO_2 exhibited two peaks during morning and evening hours of the control days due to heavy traffic and it varied from 1.2 ± 0.52 to 3.51 ± 0.62 ppbv. Natural sources of sulphur in the atmosphere comes mainly from hydrogen sulphide and dimethyl disulphide. As the solar intensity attains its maximum value during day time hours, SO_2 concentration shows relatively low level due to efficient oxidation to sulphate molecules through the oxidization of O_3 and OH radicals (Margitan, 1984). With respect to control days, the concentration of SO_2 was low during eclipse day. Fig. 4(d) shows a decline of SO_2 from 3.13 ± 0.82 to 2.58 ppbv (17.6%) with respect to control days at the maximum phase of eclipse episode. This decrease in SO_2 concentration observed during the eclipse may be one of the causes for the decrease observed in O_3 concentration. It was further observed that the concentration of SO_2 regained its same concentration as that of the control days, nearly after four hours of completion of the eclipse event.

Daily NH_3 exhibited a temporal variation with higher concentrations during early morning and late evening hours, due to the accumulation of air pollutants by lower wind speeds (Zhao *et al.*, 2016; Wang *et al.*, 2015). During control days, on diurnal basis the mixing ratios of NH_3 varied from 5.06 ± 0.38 to 6.16 ± 0.42 ppbv. During eclipse day, the concentration of NH_3 started increasing from the beginning of the eclipse, and reaches its higher concentration during the maximum phase of eclipse. With respect to control day's average concentration, NH_3 increased from 5.32 ± 0.32 to 5.92 ppbv during the maximum phase of solar obscuration. It leads to a change of 11.3% of increase in NH_3 concentration at the maximum phase of the eclipse. The night time chemical reaction may have been taking place to increase the concentration of NH_3 during the eclipse episode. This may be the prime reason for the observed enhanced concentration of NH_3 during the eclipse episode. Further, the lowering of boundary layer height during the eclipse episode may also contribute higher mixing ratio of NH_3 over the observational site. Singh *et al.* (2001); Sing and Kulshres-

Table 1. Percentage of changes observed in solar radiation, O_3, NO_2, CO, SO_2, NH_3, BTEX, temperature and relative humidity during the solar eclipse episode with respect to control days.

Time (IST)	Percentage of change in during eclipse episode with respect to control days								
	Solar radiation	O_3	NO_2	CO	SO_2	NH_3	BTEX	Temperature	R.H
8:15	−11.4	−27.1	9.1	6.5	−27.4	0.1	−8.2	−3.7	6.9
8.30	−17.0	−28.1	10.7	9.9	−29.9	1.0	−5.3	−4.5	8.6
8:45	−30.3	−35.4	18.2	12.0	−24.5	2.2	−3.6	−7.5	10.3
9:00	−40.1	−44.2	25.7	20.8	−24.8	4.6	6.2	−10.8	14.5
9:15	−65.3	−51.3	33.4	25.4	−20.6	7.8	16.7	−14.2	21.4
9:30	−93.0	−61.5	42.2	28.9	−17.6	11.3	22.6	−16.3	27.1
9:45	−73.0	−60.3	31.1	22.3	−13.2	8.6	19.9	−15.9	26.5
10:00	−60.6	−60.3	23.7	18.6	−16.1	6.2	15.6	−14.6	25.6
10:15	−48.9	−58.7	18.2	16.8	−13.6	5.9	10.7	−13.3	23.6
10:30	−27.6	−55.2	14.5	11.8	−20.8	4.8	7.4	−12.4	21.7
10:45	−25.5	−47.7	12.8	10.1	−20.7	3.9	2.3	−11.1	17.3
11:00	−23.1	−42.6	10.9	9.1	−15.0	3.1	−1.1	−10.3	13.1
11:15	−21.1	−33.5	9.5	8.5	−23.5	1.8	−3.4	−7.7	10.2

Table 2. Correlation coefficients between observed trace gases, particulate matter and meteorological parameters during eclipse episode.

Parameters	O_3	NO	NO_2	CO	SO_2	NH_3	PM_{10}	VOC's (BTEX)	Solar radiation	RH	Temp:	Wind speed
O_3	1	0.74	−0.76	−0.72	−0.84	0.93	−0.65	−0.75	0.90	−0.32	0.81	0.68
NO		1	−0.96	−0.95	−0.92	0.82	−0.92	−0.82	0.62	0.53	0.42	0.82
NO_2			1	0.93	0.94	−0.81	0.91	0.78	−0.62	−0.56	−0.41	−0.84
CO				1	0.95	−0.76	0.94	0.79	−0.57	−0.58	−0.39	−0.83
SO_2					1	−0.87	0.82	0.87	−0.71	0.94	−0.88	−0.71
NH_3						1	−0.58	−0.76	−0.78	−0.58	0.75	0.58
PM_{10}							1	0.78	−0.81	−0.67	−0.76	−0.72
VOC's (BTEX)								1	−0.60	−0.28	−0.61	−0.44
Solar radiation									1	−0.36	0.90	0.37
RH										1	−0.54	0.63
Temp:											1	0.22
Wind speed												1

tha (2012); Zhao *et al.* (2016), have reported that the concentration of NH_3 in the night is increasing in urban and rural areas.

Benzene, toluene, ethyl benzene, xylenes (BTEX) are the major hydrocarbons found in the atmosphere in the category of volatile organic compounds (VOC's) which play a vital role in the production and photochemical reaction of O_3 and other oxidants in the lower atmosphere (Sahu and Saxena, 2015; Yassaa *et al.*, 2011; Srivastava *et al.*, 2005; Sillman, 1995). VOC's are able to enhance the oxidising capacity of the atmosphere by photochemical reactions with hydroxyl radicals (OH) in the presence of NO_x (Lee *et al.*, 2002; Atkinson, 2000). At a high ratio of VOC to NO_x environment, OH will react mainly with VOC's and at a low ratio, OH will react with NO_x (Senfield and pandis, 2006). The diurnal variation of BTEX exhibited an increasing trend during late night to early morning and morning hours. Further, it shows a decreasing trend during afternoon (12:00 to 18:00 IST) hours. A similar type of variation was reported by Tiwari *et al.* (2010) in Yokohama city, Japan, Torre *et al.* (2015) in Monterrey, Mexico and Yurdakul *et al.* (2017) in Bursa, Turkey. The observation revealed the fact that the variation in total concentration of BTEX showed not much changes during eclipse period. The concentrations were found to be increased from 8.08 ±

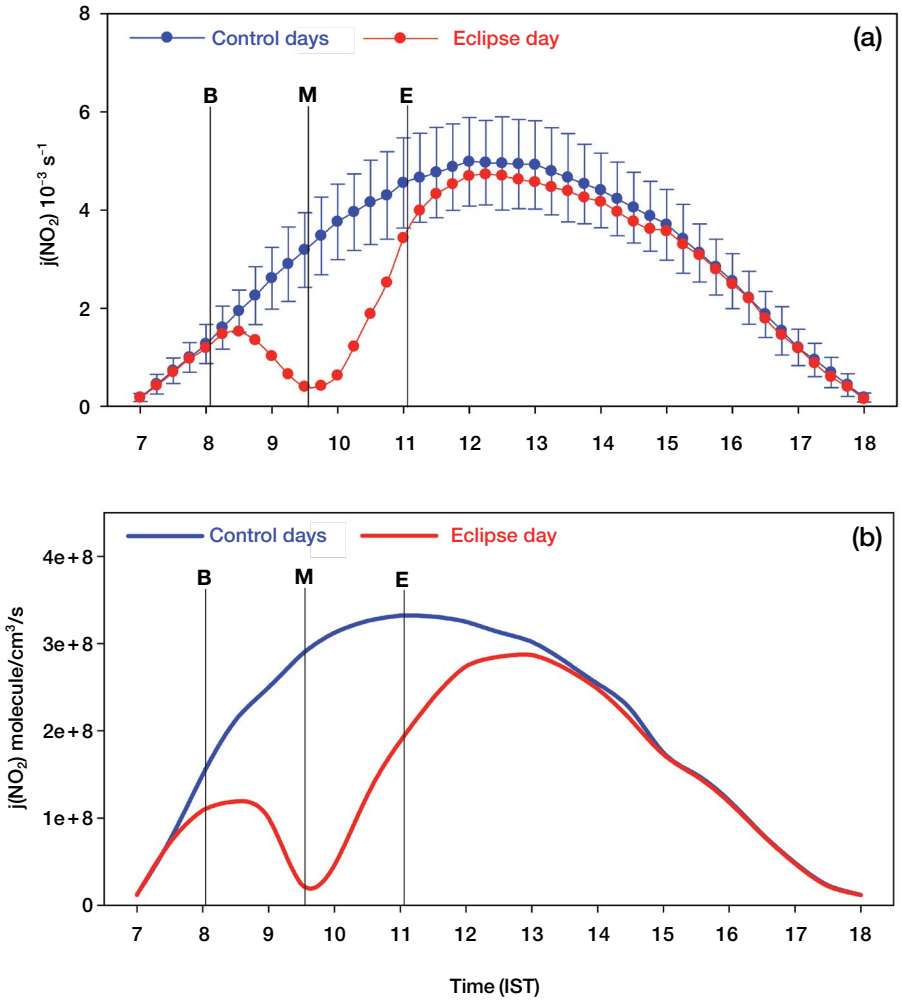

Fig. 7. Diurnal variation of (a) theoretically calculated j(NO_2), (b) Model simulated j(NO_2) for control day and eclipse day.

1.52 to 9.92 ppbv at the maximum phase of solar obscuration and this enhancement resulted a change of 22.6% with respect to control day's average value. The observed high concentrations of BTEX at the maximum phase of solar obscuration may be due to stable atmospheric condition and the absence of photochemical reactions.

3.3 Variations of Particulate Matters

Particulate Matters (PM_{10} and $PM_{2.5}$) are considered to be one of the significant components in the atmosphere, present in the form of solid and liquid suspensions. The primary source of PM in a non-industrialised location is the exhaust of automobiles (Liu *et al.*, 2015; Srimuruganandam and Nagendra, 2011; Cheng *et al.*, 2006; Latha and Badarinath, 2005). Concentration of particulate matters are depending on the variation of boundary layer height, wind speed and direction, surface solar radiation, cloud cover, sea level pressure, and precipitation. Larger boundary layer and stronger surface wind gust help speedy dispersion of particulate matters (Kim and Kim, 2020; Yang *et al.*, 2016). From night to early morning hours, atmosphere is almost stable without significant mixing which provide a favorable condition for the accumulation of particulate matters. With an increase in solar radiation in the afternoon, different environmental features mentioned above tend to accelerate the dispersion of particulate matters (Miao and Liu, 2019; Kim *et al.*, 2017). Day time variations of PM_{10} and $PM_{2.5}$ observed during eclipse day, and control days over Kannur are shown in Fig. 5. Diurnal variations of PM_{10} and $PM_{2.5}$ shows higher concentrations during morning (09:00 to 12:00 IST) and evening (16:00 to 20:00)

hours due to the peak traffic and late-night hours due the accumulation of pollutants by shallow boundary layer. During eclipse day, the concentrations of PM_{10} and $PM_{2.5}$ started increase from the beginning of the eclipse, and reaches higher concentrations during the maximum phase of eclipse. The magnitude of PM_{10} increased from 94.88 ± 18.44 to $112.4\ \mu g/m^3$ and $PM_{2.5}$ from 62.52 ± 14.04 to $69.56\ \mu g/m^3$ with percentages of increase 18.5% and 11.3%, respectively. This enhancement in PM_{10} and $PM_{2.5}$ may be influenced by the shallow boundary layer and relatively low wind speed during the eclipse.

3.4 Variations of Meteorological Parameters

In order to understand the impact of eclipse on terrestrial meteorological parameters, the daily variations of surface air temperature, relative humidity, wind speed and wind direction were analysed in detail. The required meteorological parameters were measured by using an automatic weather station (LSI LASTEM) established in the observation centre during the eclipse day and 6 control days. The diurnal variations in temperature, relative humidity, wind speed and wind direction observed on the control and eclipse days are shown in the Fig. 6. The eclipse proscribes sun light incident on the Earth's surface, and that could significantly affect the surface air temperature, and relative humidity distribution. Consequently, observed air temperature was decreased from 29.13 ± 1.35°C (with respect to control day's average) to 25.04°C with a temperature drop of 4.09°C during maximum phase of the eclipse. This temperature dip was 16.3% with a time lag of 17 minute at the full phase of the eclipse. The diurnal variation of temperature is shown in the Fig. 6(a). The reduction in temperature during eclipse episode induced a corresponding increase in relative humidity as shown in the Fig. 6(b). The relative humidity was found to be increased from $60.41 \pm 4.2\%$ (with respect to control day's average) to 76.82% during the maximum phase of solar obscuration. It resulted a change of 27.1% of increase in RH with a time lag of 18 minutes at the maximum phase of the eclipse. Namboodiri *et al.* (2011) have reported a temperature dip of 3.5°C, and 19% increase in relative humidity at a peninsular Indian coastal station (Thumba) during an eclipse on 15 January 2010.

The wind speed was found to be decreased to 36.1% with respect to control days at the maximum phase of eclipse (Fig. 6(c)), while wind direction remained unchanged during eclipse episode (Fig. 6(d)). The observed wind speed was found to decrease during the starting of eclipse, and reached its low at the full obscuration, and tended to increase and regain its normal value after completing the eclipse episode. This decrease in wind speed might be due to the freezing of atmospheric boundary due to the absence of solar radiation (Sharma *et al.*, 2010). Certainly, these deviations in weather parameters will persuade the distresses in the photochemistry of trace gases in the lower atmosphere.

The concentrations of O_3 precursor gases significantly varied during the solar eclipse episode, and the percentage of variations are listed in the Table 1. The observed NO concentrations did not show any substantial variation compared to the control days which reveal the absence of titration of O_3 leading to its destruction. From the table, it is evident that, 93% of reduction in solar radiation resulted in a decrease in temperature by 16.3% and O_3 concentration by 61.5% at the maximum phase of eclipse. At the same time NO_2, CO, and RH showed an enhancement by 42.2%, 28.9% and 27.1%, respectively.

3.5 Correlation between Air Pollutants and Meteorological Parameters

Statistical analysis (Pearson's test) is performed, and the resulted correlation coefficient between observed trace gases, particulate matters and meteorological parameters over the study area during eclipse episode is shown in the Table 2. The results point out that O_3 shows a positive correlation between NO, NH_3, solar radiation, temperature, wind speed and negative correlation with NO_2, CO, SO_2, PM_{10}, VOC's (BTEX) and relative humidity. A good positive correlation between O_3 and solar radiation ($r = 0.90$) indicates the production of O_3 by the photolysis of NO_2. Further, the correlation between O_3 and wind speed ($r = 0.68$) revealed the transport of O_3 over the observational site. Meteorological parameters such as solar radiation and temperature are in positive correlation with NO, and negative correlation with NO_2, CO, SO_2, NH_3, PM_{10} and VOC's. The negative correlations existing between wind speed with SO_2, NO_2, CO and PM_{10} point out the reduction of these pollutants by the wind. Relative humidity shows positive correlations with NO, SO_2 and negative correlations with O_3, NO_2, CO, NH_3, PM_{10}, VOC's and solar radiation. PM_{10} shows a negative correlation ($r = -0.76$) with temperature, which is due to the thermally induced decreased convection of particulate matters and condensation of VOC's. Similarly PM_{10} shows a negative corre-

lation with ($r = -0.67$) with relative humidity.

3.6 Theoretical Calculation and Model Simulation for $j(NO_2)$

Photodissociation rate coefficients (j values) is one of the vital parameters that unfolds the chemistry of air pollution. They depend on absorption cross sections, quantum yield and also the availability of solar radiation at any specific location in the atmosphere. The photolysis rate coefficient $j(NO_2)$ at a location is estimated by the equation $j(NO_2) = \int F(\lambda)\sigma(\lambda,T)\varphi(\lambda,T)d\lambda$, and the temporal variation of $j(NO_2)$ is shown in Fig. 7(a). It is found that the $j(NO_2)$ started to increase in the morning of the eclipse day, just as in the normal day. Its value gradually reduced in tune with the intensity of solar radiation in its descending and ascending phases of the eclipse and reached its minimum level during the complete obscuration. Thus, a change in the $j(NO_2)$ was found in tune with the observed variation of surface O_3. The photolysis rate coefficient $j(NO_2)$ was found to be reduced by about 87.5% during the maximum phase of the eclipse with respect to the control days. This result reveals that the photochemical production of surface O_3 from NO_2 in the presence of sunlight. Therefore, it is further realised that surface O_3 and $j(NO_2)$ found a positive relation during day time hours.

The Tropospheric Ultraviolet-Visible (TUV) model was used in the wavelength range 121–750 nm, for calculating the spectral irradiance, spectral actinic flux, and photodissociation coefficients (j-values). The TUV model simulations of $j(NO_2)$ were carried out to study the influence of solar radiation on the photochemical production of O_3 from NO_2 over the observational period. More details about the model is described by Madronich and Flocke, (1999). The model simulations were carried out by keeping all the input parameters kept constant in their normal concentrations, and by varying the intensity of solar radiation from lower to maximum. The model simulated of $j(NO_2)$ variations are shown in Fig. 7(b) for the control days and eclipse day. From the figure, it is evident, that similar to theoretical calculation, $j(NO_2)$ started to decline from its normal value of 1.19×10^8 molecules cm^{-3} sec^{-1} (beginning of eclipse at 08:06 IST) to 0.245×10^8 molecules cm^{-3} sec^{-1} (maximum phase of the eclipse at 09:26 IST). The decline in the (jNO_2) during the maximum phase of eclipse is calculated to be 91.65% with respect to control days at the same time. After completing maximum obscuration, the $j(NO_2)$ again started to increase and reaches its normal value later completing the eclipse episode at 11:05 IST.

4. CONCLUSION

A total solar eclipse provides a rare opportunity to study the effects of atmospheric changes due to the gradual dimming of solar radiation in the daytime. At Kannur, the annular solar eclipse began at 08:04 IST, reached maximum obscuration at 09:26 IST and completed at 11:05 IST. The highlights of the observation are the following:

- At the maximum phase of eclipse, solar radiation displayed a sharp decline (93%), which resulted a strident reduction (61.5%) in surface O_3 concentration due to reduced photochemical activity. The observation of total column O_3 using MICROTOPS II recorded a decrease of 31 DU in a time lag of 10 minutes from the maximum phase of the eclipse.
- Increasing trends in ground level CO and NO_2 were observed from the beginning of eclipse, and they reached their maximum concentrations during the peak of the eclipse. This enhancement in CO and NO_2 concentration were estimated to be 28.9% and 42.2%, respectively, and this increase might be due to the reduced photochemical reactions, lower boundary layer height, low wind speed and morning traffic. NO concentration remains unchanged during the maximum phase of eclipse.
- Since O_3 acts as a major oxidising agent for sulphur, consequently a decreased concentration of SO_2 was observed on the day of eclipse. With respect to control day's concentration, SO_2 decreased to 17.6% and NH_3 increased to 11.3% during the maximum phase of solar obscuration. Volatile organic compounds collectively measured BTEX was found to increase 22.6% during the maximum solar obscuration.
- Meteorological parameters such as surface air temperature, relative humidity, wind speed and wind direction were analysed on the day of eclipse. During the maximum phase of the eclipse, surface air temperature and wind speed were dropped to 16.3% and 36.1%, respectively, and relative humidity increased to 27.1%. The concentrations of PM_{10} and $PM_{2.5}$ started increasing, and attained a peak during the maximum phase of the eclipse. This upsurge leads to 18.5% and 11.3% for PM_{10} and $PM_{2.5}$ concentrations, respectively during eclipse episode.

- The variation of photodissociation coefficient j(NO_2) values were theoretically calculated from the observed data, and a reduction of 87.5% was found. This shows a good agreement with the model simulated j(NO_2) reduction of 91.65%.

The results of this study are preliminary at a polluted costal city in north Kerala during a solar eclipse. This study revealed a synoptic movement of atmospheric trace species over Kannur town, a polluted location compared to Kannur University campus in which the earlier observations were made in 2010. The observed abrupt changes in surface O_3 and other trace pollutants should be validated with more observations with the support of other prominent trace species including OH radical and organic samples to understand their role in O_3 chemistry and transport in the coming eclipse events.

ACKNOWLEDGEMENT

The authors are grateful to the Indian Space Research Organization (ISRO), Bangalore for the financial support provided through Atmospheric Chemistry, Transport, and Modeling project of Geosphere Biosphere Programme. Likewise, authors express their gratitude to Kerala State Council for Science Technology and Environment (KSCSTE) for granting financial support for the study of air pollutants over Kannur region. The authors wish to thank Dr. Shyam Lal, Physical Research Laboratory Ahmadabad for his constant inspiration and support throughout the programme. Authors express their gratitude to Smt. Anita Koyan (Environmental Engineer), and Dr. Smina CS (Assistant Scientist)of KSPCB for providing support in this study. Resmi expresses her gratitude to Dr. R. Venkatachalam (Principal) and Dr.D. Manivannan (HOD of Physics) of Erode Arts and Science College, Tamil Nadu for providing the necessary facilities and constant support. Prof. Valsaraj thanks the Charles and Hilda Roddey Distinguished Professorship in Chemical Engineering at LSU which supported the preparation of this manuscript. Authors thank the two anonymous reviewers and the Editor for their critical comments/suggestions which have helped us to improve the manuscript in the present form.

REFERENCES

Abram, J.P., Creasey, D.J., Heard, D.E., Lee, J.D., Pilling, M.J. (2000) Hydroxyl radical and ozone measurements in England during the solar eclipse of 11 August 1999. Geophysical Research Letters, 27(21), 3437–3440. https://doi.org/10.1029/2000GL012164

Amiridis, V., Melas, D., Balis, D.S., Papayannis, A., Founda, D., Katragkou, E., Giannakaki, E., Mamouri, R.E., Gerasopoulos, E., Zerefos, C. (2007) Aerosol lidar observations and model calculations of planetary boundary layer evolution over Greece during the March 2006 total solar eclipse. Atmospheric Chemistry and Physics, 7, 6181–6189. https://doi.org/10.5194/acp-7-6181-2007

Anderson, J. (1999) Meteorological changes during a solar eclipse. Weather, 54, 207–215. https://doi.org/10.1002/j.1477-8696.1999.tb06465.x

Anfossi, D., Schayes, G., Degrazia, G., Goulart, A. (2004) Atmospheric turbulence decay during the solar total eclipse of 11 August 1999. Boundary layer Meteorology, 111, 301–311. https://doi.org/10.1023/B:BOUN.0000016491.28111.43

Aplin, K.L., Harrison, R.G. (2003) Meteorological effects of the eclipse of 11 August 1999 in cloudy and clear conditions. Proceedings of Royal Society of London, 459, 353–371. https://doi.org/10.1098/rspa.2002.1042

Atkinson, R. (2000) Atmospheric chemistry of VOCs and NO_x. Atmospheric Environment, 34, 2063–2101. https://doi.org/10.1016/S1352-2310(99)00460-4

Beig, G., Gunthe, S., Jadhav, D.B. (2007) Simultaneous measurements of O_3 and its precursors on a diurnal scale at a semi urban site in India. Journal of Atmospheric Chemistry, 57, 239–253.

Bhat, G.S., Jagannathan, R. (2012) Moisture depletion in the surface layer in response to an annular solar eclipse. Journal of Atmospheric and Solar Terrestrial Physics, 80, 60–67. https://doi.org/10.1016/j.jastp.2012.02.025

Calamas, D.M., Nutter, C., Guajardo, D.N. (2019) Effect of 21 August 2017 solar eclipse on surface-level irradiance and ambient temperature. International Journal of Energy and Environmental Engineering, 10, 147–156. https://doi.org/10.1007/s40095-018-0290-8

Chakrabarty, D.K., Peshin, S.K., Srivastav, S.K., Shah, N.C., Pandya, K.V. (2001) Further evidence of total O_3 variation during the solar eclipse of 1995. Journal of Geophysical Research, 106(D3), 3213–3218. https://doi.org/10.1029/2000JD900522

Chakrabarty, D.K., Shah, N.C., Pandya, K.V. (1997) Fluctuation in column O_3 during the total solar eclipse of 24 October 1995. Journal of Geophysical Research, 24, 3001–3003. https://doi.org/10.1029/97GL03016

Cheng, Y., Ho, K.F., Lee, S.C., Law, S.W. (2006) Seasonal and diurnal variations of $PM_{1.0}$ $PM_{2.5}$ and PM_{10} in the roadside environment of Hong Kong, China. Particuology, 4, 312–315. https://doi.org/10.1016/S1672-2515(07)60281-4

Chudzynski, S., Czyzewski, A., Ernst, K., Pietruczuk, A., Skubiszak, W., Stacewicz, T., Stelmaszczyk, K., Szymanski, A., Sowka, I., Zwozdziak, A., Zwozdziak, J. (2001) Observation of O_3 concentration during the solar eclipse. Atmospheric Research, 57, 43–49. https://doi.org/10.1016/S0169-8095(00)00071-5

Dolas, P.M., Ramchandra, R., Sen, G.K., Patil, S.M., Jadhav, P.N.

(2002) Atmospheric surface-layer processes during the total solar eclipse of 11 August 1999. Boundary Layer Meteorology, 104, 445–461. https://doi.org/10.1023/A:1016577306546

Dutta, D., Kumar, V.P., Ratnam, M.V., Mohammad, S., Kumar, M.C.A., Rao, P.V., Rahaman, K., Basha, H.A. (2011) Response of tropical lower atmosphere to annular solar eclipse of 15 January 2010. Journal of Atmospheric and Solar Terrestrial Physics, 73, 1907–1914. https://doi.org/10.1016/j.jastp.2011.04.025

Eaton, F.D., Hines, J.R., Hatch, W.H., Cionco, R.M., Byer, J., Garvey, D., Miller, D.R. (1997) Solar eclipse effects observed in the planetary boundary layer over a desert. Boundary Layer Meteorology, 83, 331–346. https://doi.org/10.1023/A:1000219210055

Elizabeth, G. (2016) Satellite observations of surface temperature during the March 2015 total solar eclipse. Philosophical Transactions of the Royal Society, 374, 1–16. https://doi.org/10.1098/rsta.2015.0219

Fabian, P., Bernhard, R., Andreas, S., Herbert, W., Martin, W., Hans, S., Paul, S., Harald, B., Uwe, K., Peter, K., Joachim, R., Wolfram, B. (2001) Boundary layer photochemistry during a total solar eclipse. Meteorologische Zeitschrift, 10, 187–192. https://doi.org/10.1127/0941-2948/2001/0010-0187

Fernandez, W., Hidalgo, H., Coronel, G., Morales, E. (1996) Changes in meteorological variables in Coronel Oviedo Paraguay during the total solar eclipse of 3 November 1994. Earth Moon Planet, 74, 49–59. https://doi.org/10.1007/BF00118721

Foken, T., Wichura, B., Klemm, O., Gerchau, J., Winterhalter, M., Weidinger, T. (2001) Micrometeorological measurements during the total solar eclipse of August 11 1999. Meteorologische Zeitschrift, 10, 171–178. https://doi.org/10.1127/0941-2948/2001/0010-0171

Founda, D., Melas, D., Lykoudis, S., Lisaridis, I., Gerasopoulos, E., Kouvarakis, G., Petrakis, M., Zerefos, C. (2007) The effect of the total solar eclipse of 29 March 2006 on meteorological variables in Greece. Atmospheric Chemistry and Physics, 7, 5543–5553. https://doi.org/10.5194/acp-7-5543-2007

Fuglestvedt, J.S., Jonson, J.E., Isaksen, I.S.A. (1994) Effects of reductions in stratospheric Ozone on Tropospheric chemistry through changes in Photolysis Rates. Tellus B: Chemical and Physical Meteorology, 46, 172–192. https://doi.org/10.3402/tellusb.v46i3.15790

Gerasopoulos, E., Zerefos, C.S., Tsagouri, I., Founda, D., Amiridis, V., Bais, A.F., Belehaki, A., Christou, N., Economou, G., Kanakidou, M., Karamano, S,A., Petrakis, M., Zanis, P. (2008) The total solar eclipse of March 2006: Overview. Atmospheric Chemistry and Physics, 8, 5205–5220. https://doi.org/10.5194/acp-8-5205-2008

Girach, I.A., Nair, P.R., David, L.M., Hegde, P., Mishra, M.K., Kumar, G.M., Das, S.M., Ojha, N., Naja, M. (2012) The changes in near-surface O_3 and precursors at two nearby tropical sites during annular solar eclipse of 15 January 2010. Journal of Geophysical Research, 117, D01303, https://doi.org/10.1029/2011JD016521

Gorchakov, G.I., Kadygrov, E.N., Kortunova, Z.V., Isakov, A.A., Karpov, A.V., Kopeikin, V.M., Miller, E.A. (2008) Eclipse effects in the atmospheric boundary layer. Izvestiya Atmospheric and Oceanic Physics, 44, 100–106. https://doi.org/10.1134/S0001433808010118

Gröbner, J., Kazadzis, S., Kouremeti, N., Doppler, L., Tagirov, R., Shapiro, A.I. (2017) Spectral solar variations during the eclipse of March 20th 2015 at two European sites AIP Conference Proceedings, 1810, 080008. https://doi.org/10.1063/1.4975539

Hanna, E. (2000) Meteorological effect of the solar eclipse of 11 August 1999. Weather, 55, 430–446. https://doi.org/10.1002/j.1477-8696.2000.tb06481.x

Jokinen, T., Kontkanen, J., Lehtipalo, K., Manninen, H.E., Aalto, J., Castell, A.P., Garmash, O., Nieminen, T., Ehn, M., Kangasluoma, J., Junninen, H., Levula, J., Duplissy, J., Ahonen, L.R., Rantala, P., Heikkinen, L., Yan, C., Sipilä, M., Worsnop, D.R., Bäck, J., Petäjä, T., Kerminen, V.M., Kulmala, M. (2017) Solar eclipse demonstrating the importance of photochemistry in new particle formation. Nature Scientific Reports, 7, 45707. https://doi.org/10.1038/srep45707

Kapoor, R., Adiga, B.B., Singhal, S.P., Aggarwal, S.K., Gera, B.S. (1982) Studies on the atmospheric stability characteristics during the solar eclipse of February 16 1980. Boundary Layer Meteorology, 24, 415–419. https://doi.org/10.1007/BF00120730

Kazadzis, S., Bais, A., Blumthaler, M., Webb, A., Kouremeti1, N., Kift, R., Schallhart, B., Kazantzidis, A. (2007) Effects of solar eclipse of 29 March 2006 on surface radiation. Atmospheric Chemistry and Physics, 7, 5775–5783. https://doi.org/10.5194/acp-7-5775-2007

Kim, H.C., Kim, S., Kim, B.U., Jin, C.S., Hong, S., Park, R., Son, S.W., Bae, C., Bae, M., Song, C.K., Stein, A. (2017) Recent increase of surface particulate matter concentrations in the Seoul Metropolitan Area, Korea. Nature Scientific Report, 7, 4710. https://doi.org/10.1038/s41598-017-05092-8

Kim, S.U., Kim, K.Y. (2020) Physical and chemical mechanisms of the daily-to-seasonal variation of PM_{10} in Korea. Science of the Total Environment, 712, 136429. https://doi.org/10.1016/j.scitotenv.2019.136429

Koepke, P., Reuder, J., Schween, J. (2001) Spectral variation of the solar radiation during an eclipse. Meteorologische Zeitschrift, 10, 179–186. https://doi.org/10.1127/0941-2948/2001/0010-0179

Kolarz, P., Sekaric, J., Marinkovic, B.P., Filipović, D.M. (2005) Correlation between some of the meteorological parameters measured during the partial solar eclipse 11 August 1999. Journal of Atmospheric and Solar Terrestrial Physics, 67, 1357–1364. https://doi.org/10.1016/j.jastp.2005.07.016

Kostadinov, I., Giovanelli, G., Ravegnani, F., Bortoli, D., Petritili, A. (1999) Depolarization ratio of the zenith scattered radiation and measured NO_2 slant columns. Proceedings of Society of Photo Optical Instrumentation Engineers, 3754, 402–410.

Krezhova, D.D., Krumov, A.H., Yanev, T.K. (2008) Spectral investigations of the solar radiation during the total solar eclipse on March 29 2006. Journal of Atmospheric and Solar Terrestrial Physics, 70, 365–370. https://doi.org/10.1016/j.

jastp.2007.08.057
Krishnan, P., Kunhikrishnan, P.K., Nair, S.M., Ravindran, S., Ramachandran, R., Subrahamanyam, D.B., Ramana, M.V. (2004) Observations of the atmospheric surface layer parameters over a semi-arid region during the solar eclipse of August 11th 1999. Proceedings of Indian Academy of Science, 113, 353–363.
Kumar, A., Shukla, D.K., Kumar, A., Sarkar, S.K., Arya, B.C. (2014) Effects of the solar eclipse of 15 January 2010 on direct solar irradiances, surface ozone, NO_x, total ozone column and water vapour observed at Thiruvananthapuram, India. Mausam, 65, 128–136.
Latha, K.M., Badarinath, K.V.S. (2005) Seasonal variations of PM_{10} and $PM_{2.5}$ particles loading over tropical urban environment. International Journal of Environmental Health Research, 15, 63–68. https://doi.org/10.1080/09603120400018964
Lee, S.C., Chiu, M.Y., Ho, K.F., Zou, S.C., Wang, X. (2002) Volatile organic compounds (VOCs) in urban atmosphere of Hong Kong. Chemosphere, 48, 375–382. https://doi.org/10.1016/S0045-6535(02)00040-1
Liu, S.C., Tranier, M. (1988) Responses of the tropospheric ozone and odd hydrogen radicals to column ozone change. Journal of Atmospheric Chemistry, 6, 221–233. https://doi.org/10.1007/BF00053857
Liu, Z., Hu, B., Wang, L., Wu, F., Gao, W., Wang, Y. (2015) Seasonal and diurnal variation in particulate matter (PM_{10} and $PM_{2.5}$) at an urban site of Beijing: analyses from a 9-year study. Environmental Science and Pollution Research, 22, 627–642. https://doi.org/10.1007/s11356-014-3347-0
Madronich, S., Flocke, S. (1999) The role of solar radiation in atmospheric chemistry. The Handbook of Environmental Chemistry- Environmental Photochemistry, Boule P (Ed), Springer-Verlag Berlin Heidelberg, 2, 1–26. https://doi.org/10.1007/978-3-540-69044-3-1
Madronich, S., Granier, C. (1992) Impact of recent total ozone changes on tropospheric ozone photodissociation, hydroxyl radicals, and methane trends. Geophysical Research Letters, 19, 465–467. https://doi.org/10.1029/92GL00378
Mahapatra, P.S., Panda, S., Walvekar, P.P., Kumar, R., Das, T., Gurjar, B.R. (2014) Seasonal trends meteorological impacts and associated health risks with atmospheric concentrations of gaseous pollutants at an Indian coastal city. Environmental Science and Pollution Research, 21, 11418–11432. https://doi.org/10.1007/s11356-014-3078-2
Manchanda, R.K., Sinha, P.R., Sreenivasan, S., Trivedi, D.B., Kapardhi, B.V.N., Kumar, B.S., Kumar, P.R., Satyaprakash, U., Rao, V.N. (2012) In-situ measurements of vertical structure of O_3 during the solar eclipse of 15 January 2010. Journal of Atmospheric and Solar Terrestrial Physics, 84, 88–100. https://doi.org/10.1016/j.jastp.2012.05.011
Manohar, G.K., Kandalgaonkar, S.S., Kulkarni, M.K. (1995) Impact of a total solar eclipse on surface atmospheric electricity. Journal of Geophysical Research, 100, 20805–20814. https://doi.org/10.1029/95JD01295
Margitan, J.J. (1984) Mechanism of the atmospheric oxidation of Sulfur dioxide catalysis by hydroxyl radicals. Journal of Physical Chemistry, 88, 3314–3318. https://doi.org/10.1021/j150659a035
Miao, Y., Liu, S. (2019) Linkages between aerosol pollution and planetary boundary layer structure in China. Science of the Total Environment, 650, 288–296. https://doi.org/10.1016/j.scitotenv.2018.09.032
Mims III, F.M., Mims, E.R. (1993) Fluctuation in column O_3 during the total solar eclipse of July 11 1991. Journal of Geophysical Research, 20, 367–370. https://doi.org/10.1029/93GL00493
Muraleedharan, P.M., Nisha, P.G., Mohankumar, K. (2011) Effect of January 15 2010 annular solar eclipse on meteorological parameters over Goa India. Journal of Atmospheric and Solar Terrestrial Physics, 73, 1988–1998. https://doi.org/10.1016/j.jastp.2011.06.003
Nair, P.R., Ajayakumar, R.S., David, L.M., Girach, I.A., Mottungan, K. (2018) Decadal changes in surface ozone at the tropical station Thiruvananthapuram (8.542°N, 76.858°E), India: Effects of anthropogenic activities and meteorological variability. Environmental Science and Pollution Research, 25, 14827–14843. https://doi.org/10.1007/s11356-018-1695-x
Naja, M., Lal, S. (1997) Solar eclipse induced changes in surface O_3 at Ahmedabad. Indian Journal of Radio and Space Physics, 26, 312–318.
Naja, M., Lal, S. (2002) Surface O_3 and precursor gases at Gadanki (135°N 792°E) a tropical rural site in India. Journal of Geophysical Research, 107(D14), 1–13. https://doi.org/10.1029/2001JD000357
Namboodiri, K.V.S., Dileep, P.K., Mammen, K., Ramkumar, G., Kumar, K.N.V.P., Sreenivasan, S., Kumar, S.B., Manchanda., R.K. (2011) Effects of annular solar eclipse of 15 January 2010 on meteorological parameters in the 0 to 65 km region over Thumba India. Meteorologische Zeitschrif, 20, 635–647. https://doi.org/10.1127/0941-2948/2011/0253
Nishanth, T., Ojha, N., Kumar, M.K.S., Naja, M. (2011) Influence of solar eclipse of 15 January 2010 on surface O_3. Atmospheric Environment, 45, 1752–1758. https://doi.org/10.1016/j.atmosenv.2010.12.034
Nishanth, T., Praseed, K.M., Kumar, M.K.S., Valsaraj, K.T. (2014) Influence of ozone precursors and PM_{10} on the variation of surface O_3 over Kannur India. Atmospheric Research, 138, 112–124. https://doi.org/10.1016/j.atmosres.2013.10.022
Nymphas, E.F., Adeniyi, M.O., Ayoola, M.A., Oladiran, E.O. (2009) Micrometeorological measurements in Nigeria during the total solar eclipse of 29 March 2006. Journal of Atmospheric and Solar Terrestrial Physics, 71, 1245–1253. https://doi.org/10.1016/j.jastp.2009.04.014
Praveena, K., Kunhikrishnan, P.K., Nair, S.M., Sudha, R., Radhika, R., Subrahamanyam, D.B., Ramana, M.V. (2004) Observations of the atmospheric surface layer parameters over a semi-arid region during the solar eclipse of August 11th 1999. Proceedings of Indian Academy of Science, 113, 353–363.
Prenosil, T. (2000) The influence of the 11 August 1999 total solar eclipse on the weather over central Europe. Meteorologische Zeitschrift, 9, 351–359. https://doi.org/10.1127/metz/9/2000/351
Raman, S. (1982) Dynamics of the atmospheric boundary layer

during the 1980 total solar eclipse. Proceedings of Indian National Science Academy, 48, 187–195.

Ratnam, M.V., Kumar, M.S., Basha, G., Anandan, V.K., Jayaraman, A. (2010) Effect of the annular solar eclipse of 15 January 2010 on the lower atmospheric boundary layer over a tropical rural station. Journal of Atmospheric and Solar Terrestrial Physics, 72, 1393–1400. https://doi.org/10.1016/j.jastp.2010.10.009

Reddy, K.K., Naja, M., Ojha, N., Mahesh, P., Lal, S. (2012) Influences of the boundary layer evolution on surface O_3 variations at a tropical rural site in India. Journal of Earth System Science, 121, 911–922.

Sahu, L.K., Saxena, P. (2015) High time and mass resolved PTR-TOF-MS measurements of VOC's at an urban site of India during winter: role of anthropogenic biomass burning biogenic and photochemical sources. Atmospheric Research, 164, 84–94. https://doi.org/10.1016/j.atmosres.2015.04.021

Segal, M., Turner, R.W., Prusa, J., Bitzer, J.R., Finley, S.V. (1996) Solar eclipse effect on shelter air temperature. Bulletin of American Meteorological Society, 77, 89–99. https://doi.org/10.1175/1520-0477(1996)077<0089:SEEOSA>2.0.CO;2

Seinfeld, J.H., Pandis, S.N. (2006) Atmospheric chemistry and Physics from air pollution to climate change. John Wiley and Sons New York.

Sethuraman, S. (1982) Dynamics of the atmospheric boundary layer during the 1980 total solar eclipse. Proceedings of INSA Bulletin, 48, 187–195.

Sharma, S.K., Mandal, T.K., Arya, B.C., Saxena, M., Shukla, D.K., Mukherjee, A., Bhatnagar, R.P., Nath, S., Yadav, S., Gautam, R., Saud, T. (2010) Effects of solar eclipse on 15 January on the surface O_3, NO, NO_2, NH_3, CO mixing ratio and the meteorological parameters at Thiruvananthapuram India. Annales Geophysicae, 28, 1199–1205. https://doi.org/10.5194/angeo-28-1199-2010

Sillman, S. (1995) The use of NO_x, H_2O_2 and HNO_3 as indicators for O_3-NO_x-hydrocarbon sensitivity in urban locations. Journal of Geophysical Research, 100, 14175–14188. https://doi.org/10.1029/94JD02953

Singh, S., Kulshrestha, U.C. (2012) Abundance and distribution of gaseous ammonia and particulate ammonium at Delhi India. Biogeosciences, 9, 5023–5029. https://doi.org/10.5194/bg-9-5023-2012

Singh, S.P., Satsangi, G.S., Khare, P., Kakhani, A., Maharaj, Kumari, M., Srivastava, S.S. (2001) Multiphase measurement of atmospheric ammonia. Chemosphere, 3, 107–116. https://doi.org/10.1016/S1465-9972(00)00029-5

Srimuruganandam, B., Nagendra, S.M.S. (2011) Chemical characterization of PM_{10} and $PM_{2.5}$ mass concentrations emitted by heterogeneous traffic. Science the total Environment, 409, 3144–3157. https://doi.org/10.1016/j.scitotenv.2011.04.042

Srivastava, A., Joseph, A.E., Patil, S., More, A., Dixit, R.C., Prakash, M. (2005) Air toxics in ambient air of Delhi. Atmospheric Environment, 39, 59–71. https://doi.org/10.1016/j.atmosenv.2004.09.053

Srivastava, G.P., Pakkir, M.P.M., Balwalli, R.R. (1982) O_3 concentration measurements near the ground at Raichur during the solar eclipse of 1980. Proceedings of Indian Academy of Science, 48, 138–142.

Stoev, A., Stoeva, P., Valev, D., Kiskinova, N., Tasheva, T. (2005) Dynamics of the microclimatic parameters of the ground atmospheric layer during the total solar eclipse on August 11 1999. Geophysical Research Abstracts, 7, 10209.

Subrahamanyam, D.B., Anurose, T.J., Mohan, M., Santosh, M., Kumar, K., Kumar, N.V.P., Sijikumar, S. (2012) Impact of annular solar eclipse of 15 January 2010 on the atmospheric boundary layer characteristics over Thumba: a case study. Pure and Applied Geophysics, 169, 741–753. https://doi.org/10.1007/s00024-011-0336-9

Subrahamanyam, K.V., Ramkumar, G., Kumar, K.K., Swain, D., Kumar, S.V.S., Das, S.S., Choudhary, R.K., Namboodiri, K.V.S., Uma, K.N., Veena, S.B., John, S.R., Babu, A. (2011) Temperature perturbation in the troposphere-stratosphere at Trivandrum during the solar eclipse 2009/2010. Annales Geophysicae, 29, 275–282. https://doi.org/10.5194/angeo-29-275-2011

Szalowski, K. (2002) The effect of the solar eclipse on air temperature near the ground. Journal of Atmospheric and Solar Terrestrial Physics, 64, 1589–1600. https://doi.org/10.1016/S1364-6826(02)00134-7

Tiwari, V., Hanai, Y., Masunaga, S. (2010) Ambient levels of volatile organic compounds in the vicinity of petrochemical industrial area of Yokohama Japan. Air Quality Atmosphere and Health, 3, 65–75. https://doi.org/10.1007/s11869-009-0052-0

Torre, H.L.M., Hernandez, R.M., Domínguez, A.M. (2015) Diurnal and seasonal variation of volatile organic compounds in the atmosphere of Monterrey Mexico. Atmospheric Pollution Research, 6, 1073–1081. https://doi.org/10.1016/j.apr.2015.06.004

Tyagi, S., Tiwari, S., Mishra, A., Hopke, P.K., Attri, S.D., Srivastava, A.K., Bisht, D.S. (2016) Spatial variability of concentrations of gaseous pollutants across the national capital region of Delhi India. Atmospheric Pollution Research, 7(5), 808–816. https://doi.org/10.1016/j.apr.2016.04.008

Tzanis, C. (2005) Ground-based observations of O_3 at Athens Greece during the solar eclipse of 1999. International Journal of Remote Sensing, 26, 3585–3596. https://doi.org/10.1080/01431160500076947

Tzanis, C., Varotsos, C., Viras, L. (2008) Impacts of the solar eclipse of 29 March 2006 on the surface O_3 concentration the solar ultraviolet radiation and the meteorological parameters at Athens Greece. Atmospheric Chemistry and Physics, 7, 425–430. https://doi.org/10.5194/acp-8-425-2008

Verma, N., Satsangi, A., Lakhani, A., Kumari, K.M., Lal, S. (2017) Diurnal Seasonal and Vertical Variability in Carbon Mono$_x$ide levels at a Semi-urban Site in India. Clean Soil Air Water, 45, 1600432. https://doi.org/10.1002/clen.201600432

Vogel, B., Baldauf, M., Fiedler, F. (2001) The influence of a solar eclipse on temperature and wind in the Upper-Rhine Valley-A numerical case study. Meteorologische Zeitschrift, 10, 207–214. https://doi.org/10.1127/0941-2948/2001/0010-0207

Vyas, B.M., Saxena, A., Panwar, C. (2012) Study of atmospheric air pollutants during the partial solar eclipse on 15 January 2010 over Udaipur: A semi-arid location in Western India. Advances in Space Research, 50, 1553–1563. https://doi.org/10.1016/j.asr.2012.07.021

Wang, K.Y., Liu, C.H. (2010) Profiles of temperature response to the 22 July 2009 total solar eclipse from FORMASAT-3/COSMIC constellation. Geophysical Research Letters, 37, L01804. https://doi.org/10.1029/2009GL040968

Wang, S., Nan, J., Shi, C., Fu, Q., Gao, S., Wang, D., Cui, H., Lopez, S.A., Zhou, B. (2015) Atmospheric ammonia and its impacts on regional air quality over the megacity of Shanghai China. Nature Scientific Reports, 5, 15842. https://doi.org/10.1038/srep15842

Winkler, P., Kaminski, U., Kohler, U., Riedl, J., Schroers, H., Anwender, D. (2001) Development of meteorological parameters and total O_3 during the total solar eclipse of August 11, 1999. Meteorologische Zeitschrift, 10, 193–199. https://doi.org/10.1127/0941-2948/2001/0010-0193

Yang, Y., Liao, H., Lou, S. (2016) Increase in winter haze over eastern China in recent decades: roles of variations in meteorological parameters and anthropogenic emissions. Journal of Geophysical Research, 121, 13050–13065. https://doi.org/10.1002/2016JD025136

Yassaa, N., Ciccioli, P., Brancaleoni, E., Frattoni, M., Youcef, B.M. (2011) Ambient measurements of selected VOC's in populated and remote sites of the Sahara desert. Atmospheric Research, 100, 141–146. https://doi.org/10.1016/j.atmosres.2011.01.001

Yurdakul, S., Civan, M., Kuntasal, O., Dogan, G., Pekey, H., Tuncel, G. (2017) Temporal variations of VOC's concentrations in Bursa atmosphere. Atmospheric Pollution Research, 1–18. https://doi.org/10.1016/j.apr.2017.09.004

Zanis, P., Katragkou, E., Kanakidou, M., Psiloglou, B.E., Karathanasis, S., Vrekoussis, M., Gerasopoulos, E., Markakis, K., Poupkou, A., Amiridis, V., Melas, D., Mihalopoulos, N., Zerefos, C. (2007) Effects on surface atmospheric photooxidants over Greece during the total solar eclipse event of 29 March 2006. Atmospheric Chemistry and Physics, 7, 6061–6073. https://doi.org/10.5194/acp-7-6061-2007

Zerefos, C.S., Balis, D.S., Meleti, C., Bais, K., Tourpali, K., Kourtidis, K., Vanicek, K., Cappelani, F., Kaminski, U., Colombo, T., Stubi, R., Manea, L., Formenti, P., Andreae, M.O. (2000) Changes in surface solar UV irradiances and total ozone during the solar eclipse of August 11, 1999. Journal of Geophysical Research, 105(D21), 26463–26473. https://doi.org/10.1029/2000JD900412

Zhao, M., Wang, S., Tan, J., Hua, Y., Wu, D., Hao, J. (2016) Variation of urban atmospheric Ammonia pollution and its relation with $PM_{2.5}$ Chemical Property in Winter of Beijing, China. Aerosol and Air Quality Research, 16, 1378–1389. https://doi.org/10.4209/aaqr.2015.12.0699